Trajectory Optimization in UAV Communication System Based on User-QoS

Yikun Zou[1], Gang Wang[1(✉)], Jinlong Wang[1], Haoyang Liu[1], and Yinghua Wang[2]

[1] Communication Research Center, Harbin Institute of Technology, Harbin, China
gwang51@hit.edu.cn
[2] Nanjing Research Institute of ZTE Corporation, Nanjing, China

Abstract. Due to the mobility and flexibility of unmanned aerial vehicles (UAVs), the UAV communication networks can effectively support information transmission in the cellular networks. The purpose of this paper is to propose a scheme to ensure the fairness of information transmission for the whole users on the premise of taking into account the quality of service (QoS) of some users in the cellular networks. While considering the QoS of the users, we ensure that information transmission is not monopolized by some users by maximizing the minimum effective capacity of the whole users in the networks. By jointly optimizing user scheduling and UAV's trajectory, an iterative algorithm based on the block coordinate descent method and successive convex optimization technique is proposed. Numerical analysis results show that our proposed fairness scheme based on the QoS can improve the minimum effective capacity of the users compared with the existing schemes.

Keywords: UAV communication · User quality of service · Maximum and minimum fairness · Capacity optimization

1 Introduction

With the popularity of 5G and the grand concept of 6G, the integrated air-space-earth-sea networks have played an important role in it [1]. In the integrated air-space-earth-sea networks, unmanned aerial vehicles(UAVs), as an important part of airborne mobile wireless networks, have been widely used in a variety of military and civilian scenes [2]. Among them, the emergency communication of post-disaster rescue based on UAVs and the UAV-assisted cellular networks have been studied in depth [3]. Due to the high mobility and high flexibility, UAVs can provide high-quality line-of-sight communication links when the ground environment is not complex [4,5]. At the same time, the fixed deployment infrastructure

This work is supported in part by National Natural Science Foundation of China (No. 62071146 and No. 62071147).

Q. Guo et al. (Eds.): WiSATS 2021, LNICST 410, pp. 482–495, 2022.
https://doi.org/10.1007/978-3-030-93398-2_45

cannot meet the requirements of resource overload and high dynamic, which provides a great advantage for UAV-assisted cellular networks [6].

At present, the researches of UAV-assisted communication mainly focus on several aspects: such as UAV-assisted coverage, UAV-assisted communication, UAV-assisted Internet of Things, etc. In terms of UAV-assisted coverage, UAVs served as the aerial base stations to provide ground users with the uplink/downlink information transmission [7,8]. Lyu *et al.* focused on the efficient deployment algorithm of multi-UAV, which minimized the number of UAVs while completely covering a group of ground users in the system [7]. A cyclical time-division multiple access scheme based on the UAV communication system was proposed, in which the relationship between throughput and access delay was discussed [9]. The UAV trajectory design of a multi-UAV communication system was studied. The minimum throughput of all ground users in the downlink was maximized by optimizing multi-user communication scheduling and association as well as UAV trajectory and power control [10]. In addition, some researchers proposed various methods to improve the quality of service (QoS) of the networks in the research of the UAV-assisted cellular networks [11–13].

In this paper, we propose a UAV-assisted communication scheme based on the QoS, in which a single UAV serves each user on the ground through a cyclical time-division multiple access scheme. In this scheme, we propose several conditions to guarantee the QoS. In particular, we introduce the delay-constrained QoS index to ensure the delay requirements of the users. For the downlinks between the single-antenna UAV and the single-antenna users, we propose the optimization problem of maximizing the minimum effective capacity of each user under the delay-constrained condition to increase capacity to ensure all users' delay requirements and fairness. We consider an iterative algorithm in which UAV trajectory and user scheduling are jointly optimized and the block coordinate descent method and successive convex optimization technique are used to solve the non-convex problem. Simulation results will verify the effectiveness and convergence of the proposed algorithm.

2 System Model

As shown in Fig. 1, we consider the process of information transmission between a single UAV with a single antenna and multi-users with a single antenna on the ground. We assume that the maximum flight speed of the UAV is V_{max}, and the period T is divided into N time slots. In this paper, the three-dimensional Cartesian coordinate system is used, in which the position of the kth user and the discretized position of the UAV are expressed as $\mathbf{u}_k = [x_k, y_k, z_k]^T \in \mathbb{R}^{3\times 1}$ and $\mathbf{q}(n) = [x(n), y(n), z(n)]^T \in \mathbb{R}^{3\times 1}$ at the time $0 < t < T$. During the period T, the position of the UAV shall meet the following conditions

$$\mathbf{q}(1) = \mathbf{q}(N), \tag{1}$$

$$||\mathbf{q}[n+1] - \mathbf{q}[n]||^2 \leqslant \left(\frac{V_{max}T}{N}\right)^2, \forall n. \tag{2}$$

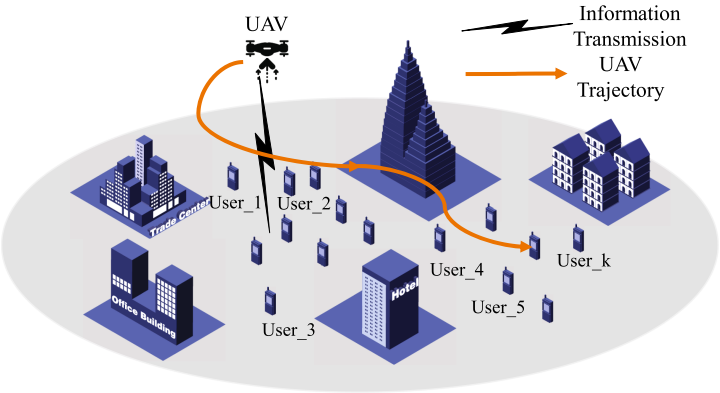

Fig. 1. UAV-enabled communication system.

Equation (1) indicates that the UAV returns to its starting point during the period T. Equation (2) states that the speed of the UAV cannot exceed its maximum flight speed V_{max} in each time slot.

In this paper, the variable $\mathbf{X} = \{x_k[n], \forall k, n\}$ is introduced when considering the connectivity between the UAV and the users. $x_k[n] = 0$ indicates that user k is not connected with the UAV in the nth time slot. $x_k[n] = 1$ indicates that user k is connected with the UAV in the nth time slot. Since the UAV can only connect to one user in each time slot, there are the following constraints

$$\sum_{k=1}^{K} x_k[n] \leqslant 1, \tag{3}$$

$$x_k[n] = \{0, 1\}. \tag{4}$$

In this paper, the communication links dominated by LoS links are adopted. In the nth time slot, the channel gain between the UAV and the kth user is expressed as

$$h_k[n] = \frac{\rho_0}{H^2 + ||\mathbf{q}[n] - u_k||^2}, \tag{5}$$

where ρ_0 represents the channel power at the reference distance $d_0 = 1$ m. The maximum transmission power of the UAV is defined as $P_{\max}$. To maximize the transmission capacity of the system of a single UAV, we assume that the UAV always transmits data at the maximum transmission power $P_{\max}$. Therefore, in the nth time slot, the received signal-to-noise ratio and the achievable rate of the kth user are

$$\gamma_k[n] = \frac{P_{\max} h_k[n]}{\sigma^2}, \tag{6}$$

$$R_k[n] = x_k[n]\log_2(1+\gamma_k[n]), \tag{7}$$

where σ^2 is the power of the additive white Gaussian noise (AWGN) at the receiver. To ensure the delay requirements in information transmission, the effective capacity based on QoS index is introduced in this paper. When the service rate sequence $R[k]$ is stationary and time-independent, the effective capacity is written as

$$C(\theta) = -\frac{1}{\theta}\log\left(\mathbb{E}\left\{e^{-\theta R[k]}\right\}\right), \tag{8}$$

where $\mathbb{E}\{\cdot\}$ represents expectation. And θ represents the QoS index. Therefore, the effective capacity of the kth user in the period T is

$$C_k = -\frac{1}{\theta_k}\log\left(\frac{1}{N}\sum_{n=1}^{N} e^{-\theta_k R_k[n]}\right). \tag{9}$$

UAV trajectory and user scheduling are $\mathbf{Q} = \{\mathbf{q}[n], \forall n\}$ and $\mathbf{X} = \{x_k[n], \forall k, n\}$, respectively. $C_{\min} = \min(C_k)$ is defined as the minimum effective capacity among the whole users, then the objective function is to maximize the minimum effective capacity among the whole users. Assuming that the location of the ground user is known, the optimization problem is expressed as

$$\max_{\mathbf{X},\mathbf{Q},C_{\min}} C_{\min}, \tag{10a}$$

$$\text{subject to} \quad -\frac{1}{\theta_k}\log\left(\frac{1}{N}\sum_{n=1}^{N} e^{-\theta_k R_k[n]}\right) \geqslant C_{\min}, \tag{10b}$$

$$||\mathbf{q}[n+1] - \mathbf{q}[n]||^2 \leqslant \left(\frac{V_{max}T}{N}\right)^2, \forall n, \tag{10c}$$

$$\mathbf{q}(1) = \mathbf{q}(N), \tag{10d}$$

$$\sum_{k=1}^{K} x_k[n] \leqslant 1, \tag{10e}$$

$$x_k[n] = \{0,1\}, \forall k, n. \tag{10f}$$

Based on (10b) and (10f), problem (10) is non-convex. The left side of (10b) is neither convex nor concave for variable $\mathbf{Q}$ or variable $\mathbf{X}$. Meanwhile, the variable $\mathbf{X}$ in (10f) is a binary discrete variable, thus (10f) has the same phenomenon with (10b). Based on this, we try to adopt the successive convex optimization technique and block coordinate descent method to solve these problems in the next section.

3 The Proposed Algorithm

To solve the problem that the variable $\mathbf{X}$ is a binary discrete variable, we can relax it into $\mathbf{X} = \{x_k[n] \in [0,1], \forall k, n\}$. Therefore, (11f) is transformed into

$0 \leqslant x_k[n] \leqslant 1, \forall k, n$. We propose an effective iterative algorithm using the block coordinate descent method to solve problem (11).

3.1 User Scheduling Optimization

For any given UAV trajectory $\mathbf{Q}$, we can simplify it into an optimization problem (11) as follows

$$\max_{\mathbf{X},\mathbf{Q},C_{\min}} C_{\min}, \tag{11a}$$

$$\text{subject to } -\frac{1}{\theta_k}\log\left(\frac{1}{N}\sum_{n=1}^{N} e^{-\theta_k x_k[n]\log_2(1+\gamma_k[n])}\right) \geqslant C_{\min}, \tag{11b}$$

$$\sum_{k=1}^{K} x_k[n] \leqslant 1, \tag{11c}$$

$$0 \leqslant x_k[n] \leqslant 1, \forall k, n. \tag{11d}$$

In the problem (11), (11a), (11c) and (11d) are convex for the variable $\mathbf{X}$, so we need to explore whether (11b) is convex for the variable $\mathbf{X}$. The first-order derivation and the second-order derivation of the effective capacity C_k in the period T with respect to any variable $x_k[n]$ are

$$C_k{}'(x_k[n]) = \frac{\beta_k[n]}{(\ln 2)^2}\frac{(1+\gamma_k[n])^{-\beta_k[n]-1}}{\sum_{n=1}^{N}(1+\gamma_k[n])^{-\beta_k[n]}}, \tag{12}$$

$$C_k{}''(x_k[n]) = \frac{1}{(\ln 2)^2 (F(x_k[n]))^2}\left[\frac{\theta_k}{\ln 2}\beta_k^2[n](1+\gamma_k[n])^{-2\beta_k[n]-2}\right.$$
$$\left. + \frac{\theta_k}{\ln 2}(1+\gamma_k[n])^{-\beta_k[n]-2}\left[(1+\gamma_k[n]) - \beta_k[n]\left(\beta_k[n]+1\right)\right]F(x_k[n])\right], \tag{13}$$

where $F(x_k[n]) = \sum_{n=1}^{N}(1+\gamma_k[n])^{-\beta_k[n]}$ and $\beta_k = \frac{\theta_k x_k[n]}{\ln 2}$. In Eq. (13), we find that the concavity and convexity of C_k for any variable $x_k[n]$ depends on the term $(1+\gamma_k[n]) - \beta_k[n]\left(\beta_k[n]+1\right)$. Since this article aims at the general users, the QoS index θ_k is usually in the range of $(0, 0.1]$. Therefore, the numerical value of $(1+\gamma_k[n]) - \beta_k[n]\left(\beta_k[n]+1\right)$ must be larger than zero, which means that C_k is convex for any variable $x_k[n]$. Finally, problem (13) is a standard convex optimization problem for the variable $\mathbf{X}$, which can be effectively solved by existing optimization tools such as CVX.

3.2 UAV Trajectory Optimization

For any given user scheduling $\mathbf{X}$, we can simplify it into an optimization problem (14) as follows

$$\max_{\mathbf{Q}, C_{\min}} \; C_{\min} \tag{14a}$$

$$\text{subject to} \;\; -\frac{1}{\theta_k}\log_2\left(\frac{1}{N}\sum_{n=1}^{N}\left(1+\frac{P_{\max}\rho_0}{\sigma^2\left(H^2+||\mathbf{q}[n]-u_k||^2\right)}\right)^{-\beta_k}\right) \geqslant C_{\min}, \tag{14b}$$

$$||\mathbf{q}[n+1]-\mathbf{q}[n]||^2 \leqslant \left(\frac{V_{max}T}{N}\right)^2, \forall n, \tag{14c}$$

$$\mathbf{q}(1)=\mathbf{q}(N). \tag{14d}$$

In problem (14), Eqs. (14a), (14c) and (14d) are all convex for the variable $\mathbf{Q}$, but the left side of (14b) is neither convex nor concave for any variable $\mathbf{q}[n]$. Further, assuming that $z_k[n]=H^2+||\mathbf{q}[n]-u_k||^2$, the effective capacity C_k in the period T for any variable $z_k[n]$ has the following first-order derivation and second-order derivation

$$C_k{}'(z_k[n]) = -\frac{\beta_k[n]\alpha}{\theta_k \ln 2}\frac{(1+\frac{\alpha}{z_k[n]})^{-\beta_k[n]-1}}{(z_k[n])^2\sum\limits_{n=1}^{N}(1+\frac{\alpha}{z_k[n]})^{-\beta_k[n]}}, \tag{15}$$

$$C_k{}''(z_k[n]) = -\frac{\alpha\beta_k[n](1+\frac{\alpha}{z_k[n]})^{-\beta_k[n]-2}}{\theta_k \ln 2(z_k[n])^4}\left[(1+\frac{\alpha}{z_k[n]})^{-\beta_k[n]}(-2z_k[n]-\alpha)\right.$$
$$\left.+\left(\left(\beta_k[n]-1\right)\alpha-2z_k[n]\right)\sum_{j=1,j\neq n}^{N}(1+\frac{\alpha}{z_k[j]})^{-\beta_k[n]}\right], \tag{16}$$

where $\alpha=\frac{P_{\max}\rho_0}{\sigma^2}$ and $\beta_k[n]=\frac{\theta_k x_k[n]}{\ln 2}$. According to Eq. (16), since the positive and negative of other terms are known, the positive and negative of the second-order derivation of C_k directly depends on $\left(\left(\beta_k[n]-1\right)\alpha-2z_k[n]\right)$. In the previous section, we mentioned that the targeted users are general users, so the value of second-order derivation of C_k must be larger than zero in the range of $(0, 0.1]$. Furthermore, C_k is convex for any variable $z_k[n]$. At the same time, we can see that $z_k[n]=H^2+||\mathbf{q}[n]-u_k||^2$ is also convex for any variable $\mathbf{q}[n]$. In this way, we can adopt successive convex optimization technique. Since the first-order Taylor expansion of an arbitrary point of an arbitrary convex function is its global lower bound, we will use the first-order Taylor expansion to approximate the original function C_k at a point $\mathbf{Z}^l$. (where $\mathbf{Q}=\mathbf{q}[\mathrm{n}],\forall\mathrm{n}\}$ is given). Assuming that the UAV trajectory $\mathbf{Q}^l=\mathbf{q}^l[\mathrm{n}],\forall\mathrm{n}\}$ and $\mathbf{Z}^l=\{H^2+||\mathbf{q}^l[n]-u_k||^2,\forall k,n\}$

are given in the lth round of the iteration, the objective function C_k can be approximated to the following form

$$\begin{aligned} C_k &= -\frac{1}{\theta_k}\log_2\left(\frac{1}{N}\sum_{n=1}^{N}\left(1+\frac{P_{\max}\rho_0}{\sigma^2 z_k[n]}\right)^{-\beta_k[n]}\right) \\ &\geqslant C_k(\mathbf{Z}^l)+C_k{}'(\mathbf{Z}^l)(\mathbf{Z}-\mathbf{Z}^l) \\ &= A-\sum_{n=1}^{N}B_k[n]\left(||\mathbf{q}[n]-u_k||^2-||\mathbf{q}^l[n]-u_k||^2\right) \\ &\triangleq C_k^{lb}, \end{aligned} \tag{17}$$

where

$$A=-\frac{1}{\theta_k}\log_2\left(\frac{1}{N}\sum_{n=1}^{N}\left(1+\frac{P_{\max}\rho_0}{\sigma^2(H^2+||\mathbf{q}^l[n]-u_k||^2)}\right)^{-\beta_k[n]}\right), \tag{18}$$

$$B_k[n]=\frac{\alpha\beta_k[n]}{\theta_k\ln 2(H^2+||\mathbf{q}^l[n]-u_k||^2)^2}\frac{(1+\frac{\alpha}{H^2+||\mathbf{q}^l[n]-u_k||^2})^{-\beta_k[n]-1}}{\sum_{n=1}^{N}(1+\frac{\alpha}{H^2+||\mathbf{q}^l[n]-u_k||^2})^{-\beta_k[n]}}. \tag{19}$$

Problem (14) is transformed into an optimization problem (20) in the following form

$$\max_{\mathbf{Q},C^r_{\min\_\mathbf{Q}}} \quad C^r_{\min\_\mathbf{Q}} \tag{20a}$$

$$\text{subject to} \quad C_k^{lb}\geqslant C^r_{\min\_\mathbf{Q}}, \tag{20b}$$

$$||\mathbf{q}[n+1]-\mathbf{q}[n]||^2\leqslant\left(\frac{V_{max}T}{N}\right)^2,\forall n, \tag{20c}$$

$$\mathbf{q}(1)=\mathbf{q}(N). \tag{20d}$$

Since (20c) and (20d) are convex for any variable $\mathbf{q}[n]$, so problem (20) is a convex optimization problem, which can be effectively solved by standard convex optimization solvers (such as CVX). It is worth noting that the target value obtained by the approximation problem (20) is the lower bound of the optimal target value of the optimization problem (14).

3.3 Global Algorithm and Convergence

According to the contents of the previous two sections, we adopt the block coordinate descent method to optimize this problem, and the proposed algorithm is as follows.

$C_{\min}\left(\mathbf{X}^l,\mathbf{Q}^l\right)$ is defined as the minimum effective capacity among all users in the lth iteration. $C^{lb}_{\min}\left(\mathbf{X}^l,\mathbf{Q}^l\right)$ is defined as the lower bound of the minimum

Algorithm 1. Block coordinate descent algorithm for problem (10).

1: **Initialize** $\mathbf{Q}^0$ and $\mathbf{X}^0$. Let $l = 0$.
2: **Repeat**
3: Given $\left\{\mathbf{Q}^l, \mathbf{X}^l\right\}$ to solve the problem (11), and define the optimal case as $\left\{\mathbf{X}^{l+1}\right\}$.
4: Given $\left\{\mathbf{Q}^l, \mathbf{X}^{l+1}\right\}$ to solve the problem (20), and define the optimal case as $\left\{\mathbf{Q}^{l+1}\right\}$.
5: Update $l = l + 1$.
6: **Until** The gain of the objective function is less than a threshold $\varepsilon > 0$.

effective capacity among all users obtained in the lth iteration. For step 3 of Algorithm 1, we can get

$$C_{\min}\left(\mathbf{X}^l, \mathbf{Q}^l\right) \leqslant C_{\min}\left(\mathbf{X}^{l+1}, \mathbf{Q}^l\right). \tag{21}$$

Since $C_{\min}\left(\mathbf{X}^{l+1}, \mathbf{Q}^l\right)$ is the optimal value in the l+1 iteration, and the optimal value after optimization must be larger than or equal to the value before optimization.

For step 4 of Algorithm 1, we can get

$$\begin{aligned} C_{\min}\left(\mathbf{X}^{l+1}, \mathbf{Q}^l\right) &\overset{(a)}{=} C_{\min}^{lb}\left(\mathbf{X}^{l+1}, \mathbf{Q}^l\right) \\ &\overset{(b)}{\leqslant} C_{\min}^{lb}\left(\mathbf{X}^{l+1}, \mathbf{Q}^{l+1}\right) \\ &\overset{(c)}{\leqslant} C_{\min}\left(\mathbf{X}^{l+1}, \mathbf{Q}^{l+1}\right), \end{aligned} \tag{22}$$

where (a) indicates that the first-order Taylor expansion is tightened at a given local point, and both the left term and the right term have the same target value. Maximizing the objective function in (b) results in that the target value after optimization must be larger than or equal to that before optimization. In (c), $C_{\min}^{lb}\left(\mathbf{X}^{l+1}, \mathbf{Q}^{l+1}\right)$ is the lower bound of $C_{\min}\left(\mathbf{X}^{l+1}, \mathbf{Q}^{l+1}\right)$. Thus, we can obtain

$$C_{\min}\left(\mathbf{X}^l, \mathbf{Q}^l\right) \leqslant C_{\min}\left(\mathbf{X}^{l+1}, \mathbf{Q}^{l+1}\right). \tag{23}$$

In the above convergence analysis, we find that although the approximate function takes the place of the objective function in the process of trajectory optimization, the overall target value is not reduced after each iteration. Since the target value of the optimization problem (10) is the upper bound of the finite value, Algorithm 1 ensures convergence. Meanwhile, the initialization scheme usually affects the convergence speed for iterative algorithms. In this section, we simplify the existing initialization scheme in [10] to make it more suitable for a single UAV. The detailed scheme is shown in Algorithm 2.

Algorithm 2. Trajectory initialization scheme for a single UAV.

1: Determine the geometric centers of multiple ground users $c_u = \frac{1}{K}\sum_{k=1}^{K} U_k$.
2: Determine the minimum radius of the UAV trajectory that can cover all users $r_u = \max_{k\in\mathcal{K}} \|u_k - c_u\|$.
3: The maximum flight radius that ensures that the UAV can return to the starting point within the cycle T $r_{\max} = \frac{V_{\max} T}{2\pi}$.
4: Determine the final flight radius of the UAV $r = \min\left(r_{\max}, \frac{r_u}{2}\right)$.
5: Determine the initial trajectory of the UAV $q^0[n] = [x + rcos\left(2\pi\frac{(n-1)}{(N-1)}\right), y + rsin\left(2\pi\frac{(n-1)}{(N-1)}\right)], \forall n$.

4 Numerical Results

In this section, we provide simulation to illustrate the effectiveness and convergence of Algorithm 1. We consider a UAV communication system with $K = 4$ ground users, where the positions of all ground users are randomly generated within an area of $1 \times 1\,\text{km}^2$. The randomly generated location of the ground users is shown in Fig. 2. The UAV is assumed to fly at a fixed altitude $H = 100\,\text{m}$. The channel power gain at the reference distance $d_0 = 1\,\text{m}$ is set to $\rho_0 = -60\,\text{dB}$. The noise power at the receiver is assumed to be $\sigma^2 = -110\,\text{dBm}$. The maximum transmission power and maximum flight speed of the UAV are $P_{\max} = 0.1\,\text{W}$ and $V_{\max} = 50\,\text{m/s}$, respectively. The convergence threshold of Algorithm 1 is $\varepsilon = 10^{-5}$.

Before analyzing the simulation, we first explain the initialization scheme of user scheduling. In this scheme, the UAV position of each time slot is connected with the nearest user, and it is guaranteed that only one user is connected to one UAV in each time slot. Figure 2 shows the flight trajectory of the UAV generated by the proposed Algorithm 1 with different periods, where the user QoS is set to $\theta = [0.1, 0.05, 0.01, 0.05]$. We find that with the increase of the flight period of the UAV, the trajectory of the UAV is also gradually increasing. This shows that the trajectory of the UAV is subject to the flight period T. Comparing the flight trajectory with a period of T=5 s and the flight trajectory with T=15 s, we can find that the longer the period of the trajectory is, the bigger the gap between the initial trajectory and the trajectory. Further, the trajectory with a longer period can arrange the flight trajectory more adaptively to maximize the minimum effective capacity in the network. From this point, we can infer that when the period is large enough, the UAV will stay directly above some users for a while to increase the minimum effective capacity, thereby increasing the overall system capacity.

Figure 3 shows the UAV flight trajectories of different user QoS, of which the two QoS schemes are $\theta_1 = [0.1, 0.05, 0.01, 0.05]$ and $\theta_2 = [0.001, 0.005, 0.08, 0.01]$. Table 1 shows the max-min effective capacity comparison of different user QoS. The higher the QoS index, the more stringent the delay requirements of the

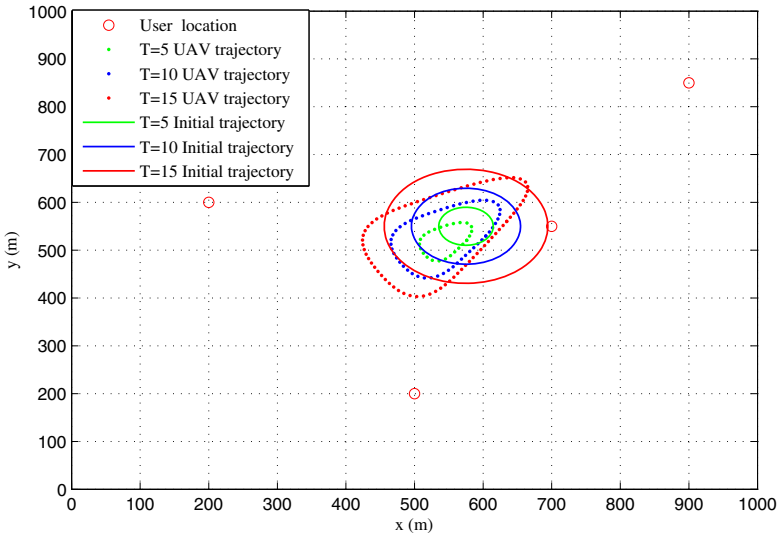

Fig. 2. The optimized trajectory of UAVs with the periods of $T = 5\,\mathrm{s}$, $T = 10\,\mathrm{s}$ and $T = 15\,\mathrm{s}$.

Table 1. Comparison of the max-min effective capacity with different user QoS

User	QoS scheme 1	QoS scheme 2
User 1	0.036618947541554	0.037037338823121
User 2	0.036618947541777	0.037037338823389
User 3	0.036618947548263	0.037037338828709
User 4	0.036618947541154	0.037037338822966

corresponding users. On the contrary, the smaller the QoS, the looser the delay requirements of users. The overall QoS of scheme 1 is larger than that of scheme 2, which shows that the users of scheme 1 have relatively strict requirements for delay. The target value of scheme 2 in Table 1 shows an increasing trend relative to scheme 1. This is because the system needs to allocate more bandwidth for users with stricter delay requirements to adapt to the effective capacity of downlink transmission. However, we strictly regulate the allocation of bandwidth, which leads to the reduction of the effective capacity of the downlink. The increase of the effective capacity of scheme 2 User 3 means that it occupies part of the effective capacity increase of other users. Comparing the trajectories corresponding to the two QoS schemes, we can see that the UAV trajectory of scheme 2 is closer to user 3 and user 4 compared to scheme 1. Since the delay requirements of user 3 and user 4 of solution 2 have become more stringent in comparison with solution 1, the UAV will approach them to meet the delay requirements.

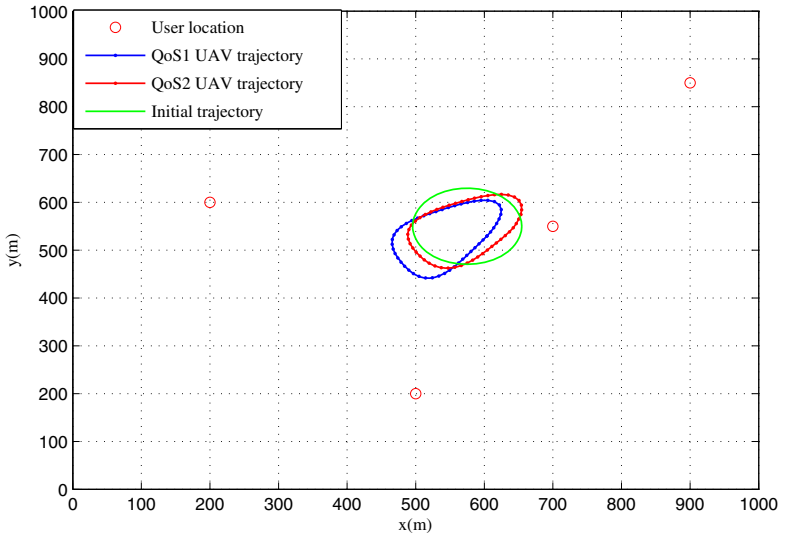

Fig. 3. The UAV optimized trajectory corresponding to different QoS when the period T=10 s.

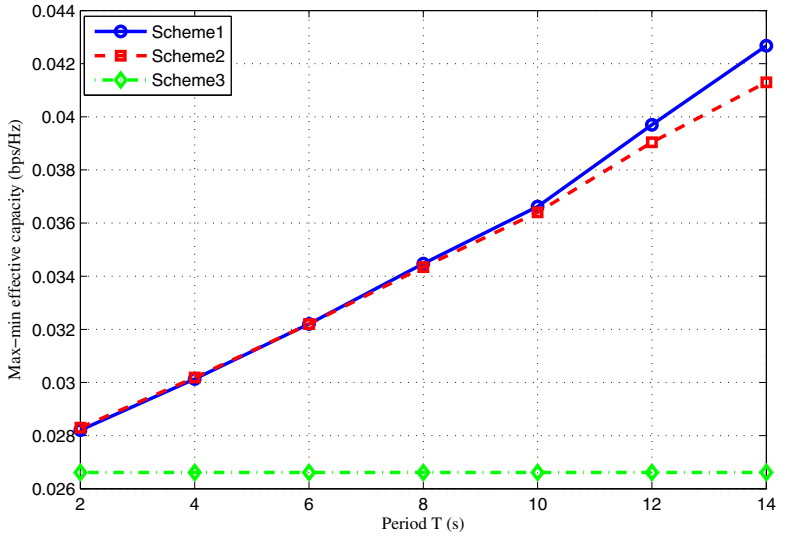

Fig. 4. The max-min effective capacity of different trajectory designs in period T.

Figure 4 shows the comparison trend of the optimal value of the proposed algorithm and the comparison algorithm in different periods of T. 1) Scheme 1: Algorithm 1 proposed in this paper, namely, joint optimization of trajectory and user scheduling; 2) Scheme 2: Optimizing the initial trajectory of user scheduling;

3) Scheme 3: UAV hovering at the geometric center. It can be seen from Fig. 4 that the target value of Scheme 3 remains unchanged and stays at a very low level. The curve of scheme 1 always stays above scheme 2. As the period increases, the gap between the two schemes gradually increases. From this, we can infer that the gap between scheme 1 and scheme 2 will increase significantly with the increase of the period. Since the flight radius of scheme 2 will not increase when the period T increases to a specific value. Even if the user scheduling is optimized, the fixed trajectory of scheme 2 will limit the communication distance between the UAV and the user to restrict the increase of the effective capacity of each user. In contrast, the UAV ensures the hovering time above each user and increases the effective capacity of each user by adaptively planning the trajectory in scheme 1 when the period T is large enough. Finally, we find that the target value in Fig. 4 is significantly smaller for two reasons: 1) the period T selected in the simulation is small, and the target value of the scheme will increase obviously with the increase of period T. 2) It is impossible for each user to connect N time slots with the UAV, and the joint optimization of user scheduling and the number of connection time slots will lead to the inability to solve the problem. Therefore, although the optimal solution obtained by scheme 1 is small, the effectiveness and convergence of Algorithm 1 can still be verified by comparing the effective capacity of all users after the compromise.

Table 2. Comparison of the maximum total capacity scheme and the max-min effective capacity scheme

User	Maximum total capacity scheme	Maxi-min effective capacity scheme
User 1	0	0.0344727255844699
User 2	0	0.0344727669486103
User 3	1	0.0344727310850233
User 4	0	0.0344728034346694

Figure 5 shows the convergence behavior of the proposed algorithm with a period of $T = 12$ s. We find that the target value will increase after each iteration and convergence will be reached quickly within about 10 iterations. Table 2 shows the user situation of maximizing the minimum effective capacity and maximizing the total capacity when the period $T = 8$ s. In the maximum total capacity scheme, the objective function is

$$C = \sum_{k=1}^{K} -\frac{1}{\theta_k} \log \left(\frac{1}{N} \sum_{n=1}^{N} e^{-\theta_k R_k[n]} \right). \tag{24}$$

It can be seen from Table 2 that the effective capacity is concentrated on one user in the maximum total capacity scheme. Since the goal is to maximize the total capacity, the UAV will find the user with the largest effective capacity in the iterative process, and then hover over the user to maximize the total system capacity. This behavior is fatal to other users' information transmission. The effective

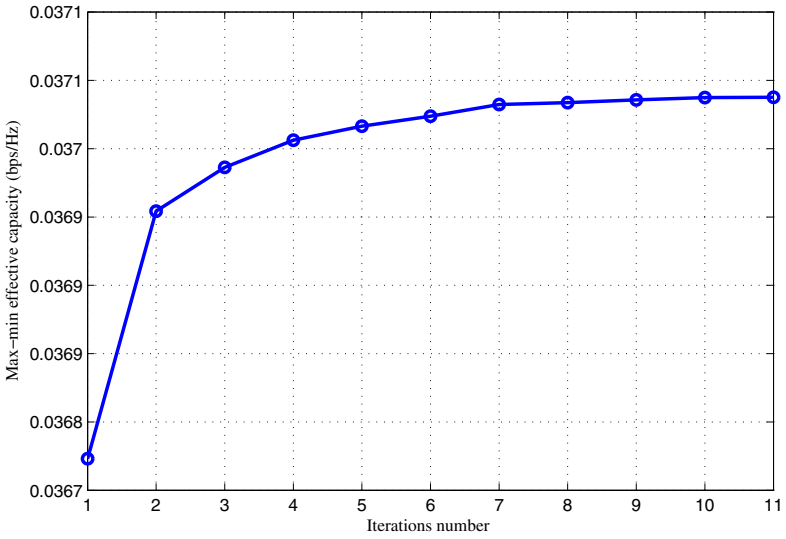

Fig. 5. Convergence behavior of proposed Algorithm 1.

capacity of each user corresponding to the objective function mentioned in this paper is very balanced, with a maximum difference of $7.78501995 \times 10^{-8}$ bps/Hz. It is verified that this paper guarantees the fairness of users. It is worth noting that the fairness of users comes at the expense of reducing the total effective capacity.

5 Conclusion

This paper studied the fairness of information transmission among users in UAV communication systems based on QoS. The main goal of this paper was to design an effective scheme for jointly optimizing user scheduling and UAV trajectory. The proposed scheme could satisfy different users' QoS requirements while ensuring that a single user could not monopolize information transmission to indirectly promote the fairness of information transmission. To this end, we proposed an iterative algorithm that adopted the block coordinate descent method and successive convex optimization technology. Compared with the circular trajectory scheme and fixed-point trajectory scheme, the convergence and effectiveness of the proposed algorithm were verified.

References

1. Cao, X., Wu, C., Lan, J., Yan, P., Li, X.: Vehicle detection and motion analysis in low-altitude airborne video under urban environment. IEEE Trans. Circuits Syst. Video Technol. **21**(10), 1522–1533 (2011)

2. Zhang, S., Liu, J., Sun, W.: Stochastic geometric analysis of multiple unmanned aerial vehicle-assisted communications over Internet of Things. IEEE Internet Things J. **6**(3), 5446–5460 (2019)
3. Liu, M., Yang, J., Gui, G.: DSF-NOMA: UAV-assisted emergency communication technology in a heterogeneous Internet of Things. IEEE Internet Things J. **6**(3), 5508–5519 (2019)
4. Jiang, B., Yang, J., Xu, H., Song, H., Zheng, G.: Multimedia data throughput maximization in Internet-of-Things system based on optimization of cache-enabled UAV. IEEE Internet Things J. **6**(2), 3525–3532 (2019)
5. Yao, H., Wang, L., Wang, X., Lu, Z., Liu, Y.: The space-terrestrial integrated network: an overview. IEEE Commun. Mag. **56**(9), 178–185 (2018)
6. Jeong, S., Simeone, O., Kang, J.: Mobile edge computing via a UAV-mounted cloudlet: optimization of bit allocation and path planning. IEEE Trans. Veh. Technol. **67**(3), 2049–2063 (2018)
7. Lyu, J., Zeng, Y., Zhang, R., Lim, T.J.: Placement optimization of UAV-mounted mobile base stations. IEEE Commun. Lett. **21**(3), 604–607 (2017)
8. Zeng, Y., Zhang, R., Lim, T.J.: Throughput maximization for UAV-enabled mobile relaying systems. IEEE Trans. Commun. **64**(12), 4983–4996 (2016)
9. Lyu, J., Zeng, Y., Zhang, R.: Cyclical multiple access in UAV-aided communications: a throughput-delay tradeoff. IEEE Wirel. Commun. Lett. **5**(6), 600–603 (2016)
10. Wu, Q., Zeng, Y., Zhang, R.: Joint trajectory and communication design for multi-UAV enabled wireless networks. IEEE Trans. Wirel. Commun. **17**(3), 2109–2121 (2018)
11. Zhang, X., Cheng, W., Zhang, H.: Heterogeneous statistical QoS provisioning over airborne mobile wireless networks. IEEE J. Sel. Areas Commun. **36**(9), 2139–2152 (2018)
12. Zhu, S., Gui, L., Cheng, N., Sun, F., Zhang, Q.: Joint design of access point selection and path planning for UAV-assisted cellular networks. IEEE Internet Things J. **7**(1), 220–233 (2020)
13. Bejaoui, A., Park, K., Alouini, M.: A QoS-oriented trajectory optimization in swarming unmanned-aerial-vehicles communications. IEEE Wirel. Commun. Lett. **9**(6), 791–794 (2020)